

The effect of radiation pressure on dusty absorbing gas around AGN

A.C. Fabian¹, R.V. Vasudevan¹ and P. Gandhi²

¹Institute of Astronomy, Madingley Road, Cambridge CB3 0HA

²RIKEN Cosmic Radiation Lab, 2-1 Hirosawa, Wakoshi, Saitama 351-0198, Japan

2 March 2022

ABSTRACT

Many Active Galactic Nuclei (AGN) are surrounded by gas which absorbs the radiation produced by accretion onto the central black hole and obscures the nucleus from direct view. The dust component of the gas greatly enhances the effect of radiation pressure above that for Thomson scattering so that an AGN which is sub-Eddington for ionized gas in the usual sense can appear super-Eddington for cold dusty gas. The radiation-pressure enhancement factor depends on the AGN spectrum but ranges between unity and about 500, depending on the column density. It means that an AGN for which the absorption is long-lived should have a column density $N_{\text{H}} > 5 \times 10^{23} \lambda \text{ cm}^{-2}$, where λ is its Eddington fraction $L_{\text{bol}}/L_{\text{Edd}}$, provided that $N_{\text{H}} > 5 \times 10^{21} \text{ cm}^{-2}$. We have compared the distribution of several samples of AGN – local, CDFS and Lockman Hole – with this expectation and find good agreement. We show that the limiting enhancement factor can explain the black hole mass – bulge mass relation and note that the effect of radiation pressure on dusty gas may be a key component in the feedback of momentum and energy from a central black hole to a galaxy.

Key words: galaxies: nuclei - galaxies: ISM - quasars: general - radiative transfer

1 INTRODUCTION

Active Galactic Nuclei are powered by accretion onto a central massive black hole. The gas surrounding the nucleus, some of which provides the fuel for the accretion process, often obscures it from direct view. Indeed, the hard shape of the spectrum of the X-ray Background argues that most accretion onto galactic nuclei is obscured (Fabian & Iwasawa 1999). This is confirmed by deep Chandra and XMM-Newton imaging of the Sky with many AGN found to lie behind a column density of $10^{22} - 10^{23} \text{ cm}^{-2}$ or more (Giacconi et al. 2002; Brandt & Hasinger 2005).

Much of the obscuring material must lie within the inner 100 pc, or its total mass would be prohibitive (see Maiolino & Risaliti 2007 for a review). It is therefore part of the inner bulge of the host galaxy. Stars can also form from this gas, giving a nuclear starburst. The gas is subject to the radiation pressure of the AGN, and can be ejected from the bulge if the nucleus becomes too bright. Such AGN feedback may thereby remove the gas which fuels the nucleus and from which new stars form, so terminating the growth of both the central black hole and its host bulge. Simple calculations of when this occurs (Fabian 1999; Fabian et al. 2002; King 2003, Murray et al. 2005; Fabian et al. 2006) lead to the following relation between the mass of the black hole M_{BH} and the velocity dispersion of the bulge σ :

$$M_{\text{BH}} = \frac{f\sigma^4}{\pi G^2 m_{\text{p}}} \sigma_{\text{T}}. \quad (1)$$

Assuming a gas fraction $f \sim 0.1$, this gives an $M_{\text{BH}} - \sigma$ relation in

good agreement with observations (Kormendy & Richstone 1995; Magorrian et al. 1998; Gebhardt et al. 2000; Ferrarese et al. 2001).

The limit when radiation pressure ejects mass is an effective Eddington limit relying on absorption of radiation by dust, not electron scattering. The radiation pressure is amplified or boosted by a factor A which is the ratio of the effective, frequency weighted, absorption cross section for dusty gas, σ_{d} to that for electrons alone: σ_{T} .

$$A = \frac{\sigma_{\text{d}}}{\sigma_{\text{T}}}. \quad (2)$$

The dust absorption is greatest in the UV and the value of A depends on the spectrum of the AGN. The X-ray emission from the nucleus ensures that the gas and dust remain weakly ionized, and are effectively coupled by Coulomb forces so that pressure on the grains is shared with the surrounding gas.

Boost factors computed for a standard AGN spectrum, using the radiation code CLOUDY are shown in Fabian et al. (2006) and Fig. 1. They range from several hundred for low column densities and drop as the column density of gas increases until they approach unity when the gas becomes Compton thick, i.e. $N_{\text{H}} \sim 1/\sigma_{\text{T}} = 1.5 \times 10^{24} \text{ cm}^{-2}$. Under the assumptions used, the main reduction of A with column density N_{H} is merely due to the increased column acting as a dead weight since the UV part of the spectrum is used up after traversing a column of a few 10^{21} cm^{-2} . The outer 'dead weight' is then pushed by the inner gas which experiences the full force of the radiation.

In this paper we explore further the implications of the boost factor on the limit to the column density of dusty gas that can re-

arXiv:0712.0277v1 [astro-ph] 3 Dec 2007

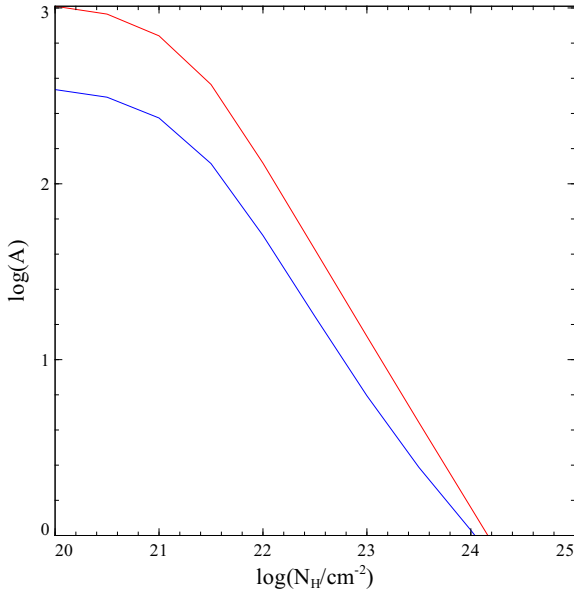


Figure 1. The radiation pressure boost factor A for dusty gas shown as a function of column density N_{H} . The continuum spectrum is assumed to be that of high and low Eddington ratio objects (from Vasudevan & Fabian (2007)) for the upper and lower lines, respectively.

main close to an AGN without being ejected by radiation pressure. The key feature is to cast the inverse of the boost factor as the (classical) Eddington ratio λ :

$$A^{-1} = \frac{L_{\text{Bol}}}{L_{\text{Edd}}} = \lambda. \quad (3)$$

A cloud is long lived if $A\lambda < 1$. If the boost factor for a particular cloud is 100 then it will be blown away when the Eddington ratio exceeds 1/100. This determines a relation between the column density of long-lived absorbing gas close to a nucleus and its Eddington ratio.

Pier & Krolik (1992) have previously noted the role of the Eddington ratio when explaining the geometrical thickness of the torus around AGN by the action of radiation pressure. Hönig & Beckert (2007) have estimated the effective Eddington limit for a torus around an AGN considering both smooth and clumpy dust distributions.

Previous work on the luminosity dependence of absorption has found that the incidence of absorption drops with luminosity (Ueda et al. 2003; La Franca et al. 2005, but see Dwelly & Page 2006, Treister & Urry 2005). The ‘receding torus’ model (Lawrence 1991; Simpson 1998) is often invoked to explain why quasars may show less absorption. In that model the reduction in absorbed objects is attributed to (heating) destruction of dust within the inner regions of a torus of absorbing gas surrounding the nucleus.

Here we consider the relation between luminosity and absorption from the point of view of the effective Eddington limit on dusty gas.

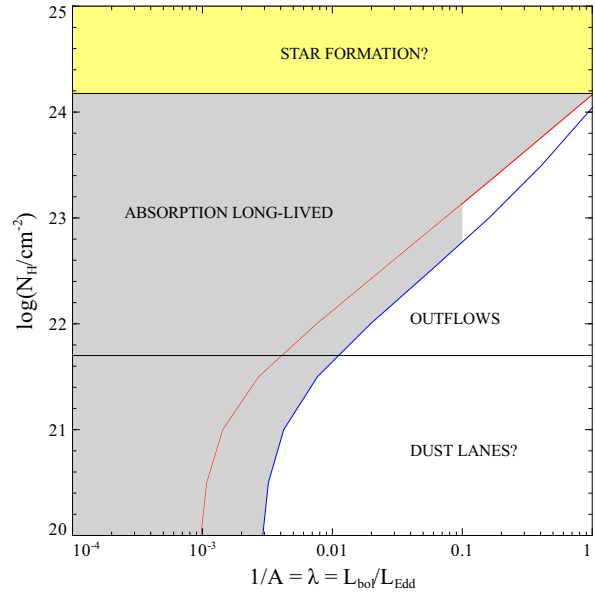


Figure 2. Fig. 1 replotted in terms of column density versus $1/A$. Long-lived absorption from clouds near the centre of the galaxy should occur in the shaded region. Absorption from clouds and dust lanes can occur at higher values of λ progressively further out. High column densities there would require prohibitive gas masses so we restrict such a region to $N_{\text{H}} < 5 \times 10^{21} \text{ cm}^{-2}$, marked by a horizontal line.

2 THE RELATION BETWEEN BOOST FACTOR AND EDDINGTON RATIO

We determine the boost factor A as detailed in Fabian et al. (2006) using CLOUDY and AGN spectral energy distributions obtained by Vasudevan & Fabian (2007). A is obtained from absorption only (the input spectrum minus the transmitted one) and assumes that the gas is optically thin to the infrared radiation thereby produced. Trapping of radiation is assumed to be negligible and the ionization parameter $\xi = L/nr^2$ is arranged to be about 10 (thereby fixing the gas density for a given incident AGN flux). Vasudevan & Fabian (2007) find that the UV – X-ray spectral energy distributions (SEDs) of AGN depend on Eddington ratio, with much more ionizing radiation – and therefore higher boost factors – occurring at higher λ . We adopt mean SEDs for high (> 0.1) and low (< 0.1) λ when computing A as a function of absorption column density. N_{H} is plotted against $\lambda = A^{-1}$ in Fig. 2. The drift velocity of the grains relative to the gas is computed by CLOUDY and found to be low (about 0.1 km s^{-1} where most of the radiative force is applied) justifying our assumption that the dust and gas are coupled.

Long-lived absorbing clouds can survive against radiation pressure in the shaded region of the Figure. Clouds to the right of the dividing line, in the unshaded part, see the nucleus as above the effective Eddington luminosity and are thus ejected. Objects found in this region should be experiencing outflows and absorption may be transient or variable. The Compton-thick objects never see the source as exceeding the Eddington luminosity and so can be long-lived at all Eddington ratios less than unity. Gas clouds in this regime are more likely to change because of star formation.

Absorbed objects in the unshaded part at higher Eddington ratio should exhibit outflows, or the absorbing gas be far away from the nucleus where the retaining gravitational mass is much larger.

They could for instance be associated with dust lanes, as envisaged by Matt (2000). Such absorption cannot be too large or the gas mass required would be prohibitive. We show, for example, a limit at $N_{\text{H}} = 5 \times 10^{21} \text{ cm}^{-2}$ in Fig. 2.

Our prediction is therefore that absorbed objects should lie above the approximate dividing line given by $N_{\text{H}} > 5 \times 10^{23} \lambda \text{ cm}^{-2}$, provided that $N_{\text{H}} > 5 \times 10^{21} \text{ cm}^{-2}$.

3 COMPARISON WITH DATA

The simple model described above predicts that most highly-obscured AGN will be observed to have an intrinsic column density placing them in the shaded region of Fig. 2.

In order to test our model, we have examined the absorption and black hole mass of several samples. The first is a composite low redshift sample consisting of the Markwardt et al. (2005) sample of AGN detected by the Burst Alert Telescope (BAT) on the *SWIFT* satellite, and the Dadina (2007) sample of Seyfert nuclei observed by the *BeppoSAX* satellite. The former is an all-sky, hard-X-ray-flux limited sample in the energy range 14–195 keV where detection should be independent of column density, provided the source is not too Compton thick. The latter study presents an atlas of X-ray spectra for 39 Seyfert I and 42 Seyfert II nuclei over the energy range 2–100 keV. All objects in the combined sample have redshifts below 0.05. Black hole masses are estimated from velocity dispersions using the $M - \sigma$ relation of Tremaine et al. (2002). Velocity dispersions were obtained from the HyperLEDA online database. We obtained 2–10keV luminosities from the Tartarus¹ database of *ASCA* observations, as it was not possible to extrapolate a 2–10keV luminosity from the *SWIFT* luminosities provided in Markwardt et al. (2005) without a value for the photon index Γ . Finally, we convert to a bolometric luminosity using the Eddington-ratio-dependent bolometric correction scheme of Vasudevan & Fabian (2007), using the black hole mass to estimate the Eddington ratio λ , and assume that the emission is isotropic. We obtained velocity dispersions, and thus calculated masses, for 23 objects in the composite sample. The results for this sample are shown in Fig. 3.

In this Figure we see one object with a large column density and high Eddington ratio in the unshaded region. This is NGC 3783, and the absorption is part of an outflowing warm absorber (Kaspi et al. 2001). The 3 objects with $22 > \log N_{\text{H}} > 21$ (just below the horizontal line) are, in order of increasing λ , IC 4329A, which has an outflow and is seen almost edge on so absorption may be from a distant dust lane (Markowitz et al. 2006); NGC3516, which has variable absorption and an outflow (Markowitz et al. 2007); and 3C120, which has a soft excess in XMM spectra (Ballantyne et al. 2004) so may have N_{H} overestimated in the value tabulated by Markwardt et al (2005) used in Fig. 3.

We then used deeper samples. First we use the Chandra Deep Field South results of Tozzi et al. (2006). These authors provide values for the column density N_{H} for each AGN together with intrinsic X-ray luminosities. We calculate black hole mass estimates using K-band magnitudes from Szokoly et al. (2004) and the $M_{\text{BH}} - L_{\text{K}}$ relation of Marconi & Hunt (2003). We impose a redshift cut, requiring our objects to lie between redshifts $0.5 < z < 1.0$. We attempt to account for some evolution in the $M_{\text{BH}} - L_{\text{K}}$

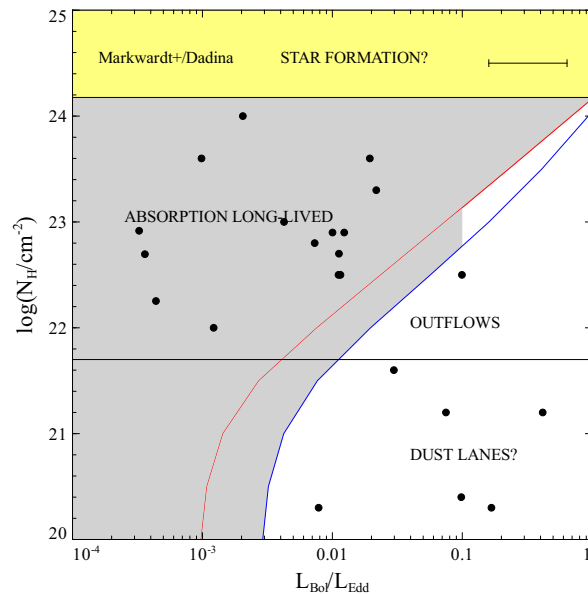


Figure 3. Objects from the samples taken from the work of Markwardt et al. (2005) and Dadina (2007) plotted on the $N_{\text{H}} - \lambda = L_{\text{Bol}}/L_{\text{Edd}}$ plane. An estimate of the uncertainty in $\lambda = L_{\text{Bol}}/L_{\text{Edd}}$ is shown by the bar at top right.

relation between that epoch and our own by incrementing the K-band magnitudes by unity before using the relation (i.e. accounting for fainter bulge luminosities for the same central black hole mass in the past). This is broadly consistent with the evolution expected from van der Wel et al. (2006), assuming negligible evolution in the ratio $M_{\text{stellar}}/M_{\text{BH}}$. This produces estimates for M_{BH} in line with other measures. Using bolometric corrections as for the local sample, we estimate the Eddington ratios as before. This sample yields 77 objects for which mass estimates could be obtained. The results are shown in Fig. 4 (top); objects with negligible column density are marked nominally as having an upper limiting N_{H} of 10^{21} cm^{-2} (downward arrows). The range of Eddington ratios that we find for the CDFS sources is comparable to that found independently by Babić et al. (2007).

Finally we used the Lockman Hole results of Mainieri et al. (2002) and Mateos et al. (2005). Mass estimates were calculated using K-band magnitudes from Mainieri et al. (2002), whereas X-ray luminosities and column densities were taken from Mateos et al. (2005) and bolometric corrections as before. The redshift range used was the same as for the CDFS sample. There were 13 objects satisfying these criteria, and the results are shown in Fig. 4 (bottom).

The results from the deeper samples are qualitatively similar to the low redshift sample. For all three samples we find, as predicted, that most objects lie within the shaded region. Note that since Chandra probes deeper than XMM, most of the CDFS objects are at a lower value of λ than those in the Lockman Hole.

We show relatively conservative estimates for the uncertainties involved to provide some indication of the validity of our results. In the local Seyfert sample (Fig. 3), we use published errors on velocity dispersions and assume errors of 10 per cent on the Tartarus X-ray fluxes and also on the values of N_{H} provided. For the distant samples, we assume errors of 20 per cent on both K-band and 2–10 keV luminosities. In the case of the K-band, we note that

¹ <http://astro.ic.ac.uk/Research/Tartarus/>

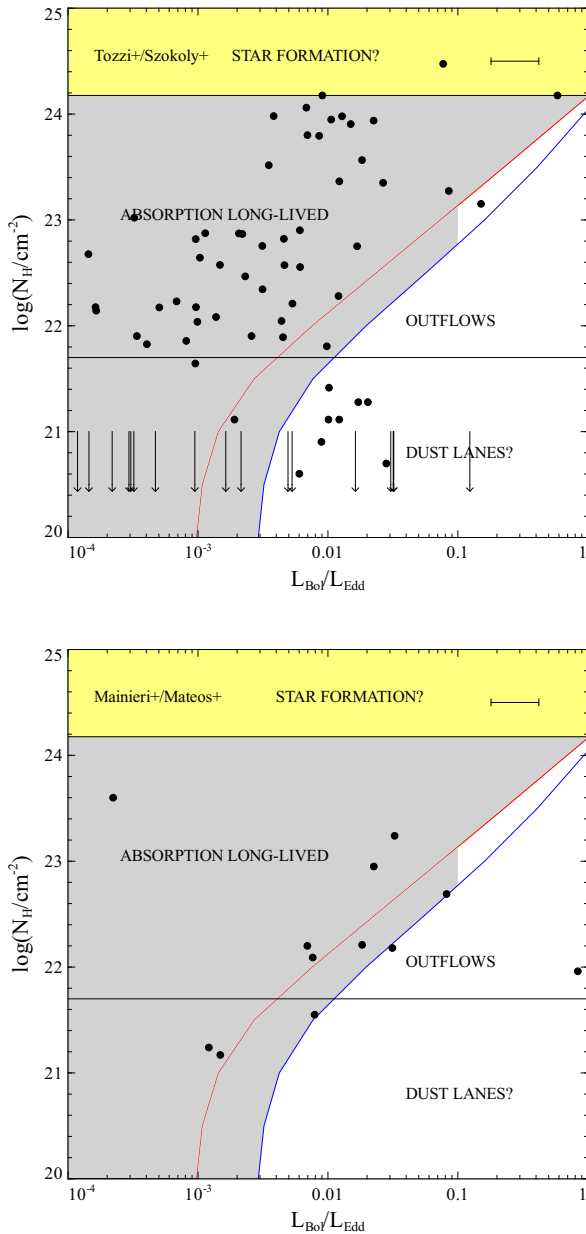


Figure 4. The $N_{\text{H}} - \lambda = L_{\text{BoL}}/L_{\text{Edd}}$ plane with objects from the CDFS (top) using data from Tozzi et al. (2006) and Szokoly et al. (2004), and the Lockman Hole (bottom) using data from Mainieri et al. (2002) and Mateos et al. (2005). There is one point missing from each plot with $\lambda < 10^{-4}$.

Marconi and Hunt (2003) identify errors of ± 0.1 on K-band magnitudes, translating to ~ 10 per cent in luminosity; we suggest that the 20 per cent value used here is therefore a reasonably ‘safe’ estimate of the error. For the X-ray band, one may expect variability to introduce significant uncertainties, but we suggest that 20 per cent error is again relatively conservative for most objects. Such error estimates lead to uncertainties of around ~ 40 per cent in the Eddington ratios; however, this is small enough to clearly differentiate those lying within the shaded regions on Figs. 3 and 4 from those which are not. The typical error in λ under these assumptions is shown in Figs. 3 and 4 by the bar in the top right.

4 DISCUSSION

We see from the plots that most absorbed AGN with column densities $N_{\text{H}} > 10^{22} \text{ cm}^{-2}$ have an Eddington ratio $\lambda < 0.1$, as expected if radiation pressure on dusty gas is important. The observed objects are sub-Eddington in terms of radiation pressure on dusty gas and so the absorbing gas may be long-lived. The line defining the effective Eddington limit in the plots is determined for the mass of the black hole only. It shifts to the right (higher values of λ) if larger masses associated with the stellar bulge are also involved. Since the lines drawn seem to apply to the samples, most of the absorbing gas must be at small radii (much less than 100 pc). The agreement between the expected location of absorbed AGN and the observed locations provides support for the idea that radiation pressure acts to blow gas away from galaxy bulges. If the radiation is isotropic then it can stem the growth of both inner bulge and black hole.

The inner gas directly exposed to the radiation pressure may be unstable to clumping (Blumenthal & Mathews 1979; Höning & Beckert 2007), the details of which will not be pursued here. Most of the long-lived gas at column densities above 10^{22} cm^{-2} is shielded by the inner gas and so need not be clumped.

After blowing away the gas, AGN may decline in luminosity so creating unabsorbed sources at low Eddington ratios. There is also some uncertainty in the boundary between the various regions of the diagrams due to factors such as source variability and clumpiness in the absorption. The fact that most sources avoid the region of our diagrams above $N_{\text{H}} \sim 5 \times 10^{21} \text{ cm}^{-2}$ and to the right of the radiation pressure line demonstrates that variability is not very important.

Lower levels of absorption below 10^{22} cm^{-2} can be long-lived at large radii in a galaxy, since the relevant gravitating mass there is due to the black hole and the bulge. The radiation limit in our Figures shifts to the right by a factor of $M_{\text{bulge}}/M_{\text{BH}}$ with all gas above the line bound to the bulge. The maximum boost A that can be obtained from radiation pressure on dusty gas is $\sigma_{\text{d}}/\sigma_{\text{T}} \sim 500$ which means that the black hole is above the effective Eddington limit for the whole bulge if $M_{\text{BH}}/M_{\text{bulge}} > 1/500$.

Consequently we envisage a scenario where a black hole smothered in gas could grow in a bulge in stages. It pushes the gas out to a distance in the bulge where the mass within that radius is 500 times the black hole mass. (The boost factor increases as the column density decreases, so once gas starts to move outward it continues to do so, see Fig. 1 and Fabian et al. 2006) After the accretion disk empties, the AGN switches off. If the bulge mass within the radius to which the gas was pushed exceeds 500 times the mass of the black hole, then the gas falls back in and the cycle repeats. Through accretion, the black hole mass and thus luminosity increases each cycle until it is unable to retain the gas and it is pushed right out of the bulge. At this point

$$M_{\text{BH}}/M_{\text{bulge}} \sim \sigma_{\text{T}}/\sigma_{\text{d}} \sim 1/500, \quad (4)$$

similar to the value found by Marconi & Hunt (2004) from correlating the observed properties of galaxies.

Star formation from the gas in the galaxy during these cycles presumably leads to the bulge mass – velocity dispersion (Faber-Jackson) relation required such that equations (1), which acts locally, and (2), which acts globally, agree.

For much of the ‘cycling scenario’ envisaged above, the only acceptable range for bright unabsorbed objects would be at high Eddington ratios. From a large sample of AGN detected in

their AGN and Galaxy Evolution Survey (AGES), Kollmeier et al. (2006) find $\lambda \sim 0.2$. An important result from their survey is that they should have been sensitive to unabsorbed AGN with lower Eddington ratios, but found none. This could in part be a selection effect due to absorption since the Chandra X-ray observations used are short, about 5 ks, which means that they are most sensitive to bright unabsorbed objects. The discussion of emission line strength for high and low Eddington ratio AGN from Vasudevan & Fabian (2007) could also be of particular relevance here, again implying that higher Eddington ratio AGN would be systematically favoured. The detected objects are in the unshaded part of our diagram, so have high λ .

5 SUMMARY

Absorbed AGN are most commonly found at low Eddington ratios such that they are sub-Eddington for dusty gas. This agrees with the hypothesis that radiation pressure acting on dust is important in removing gas from galaxy bulges. In turn this leads to $M_{\text{BH}} - \sigma$ and $M_{\text{BH}} - M_{\text{bulge}}$ relations similar to those observed.

Studies seeking to examine the evolution of absorbed AGN will need to include the dependence on Eddington ratio.

6 ACKNOWLEDGMENTS

We acknowledge Gary Ferland for the use of his code CLOUDY and for discussions. We thank Silvia Mateos and Vincenzo Mainieri for helpful suggestions and information on the data presented in their papers. ACF thanks The Royal Society for support, RV acknowledges support from the UK Science and Technology Funding Council (STFC) and PG acknowledges a Fellowship from the Japan Society for the Promotion of Science (JSPS). This research has made use of the Tartarus (Version 3.2) database, created by Paul O'Neill and Kirpal Nandra at Imperial College London, and Jane Turner at NASA/GSFC. Tartarus is supported by funding from STFC (PPARC), and NASA grants NAG5-7385 and NAG5-7067.

REFERENCES

- Babić A., Miller L., Jarvis M. J., Turner T. J., Alexander D. M., Croom S. M., 2007, *A&A*, 474, 755
 Ballantyne D. R., Fabian A. C., Iwasawa K., 2004, *MNRAS*, 354, 839
 Blumenthal G. R., Mathews W. G., 1979, *ApJ*, 233, 479
 Brandt W. N., Hasinger G., 2005, *ARA&A*, 43, 827
 Dadina M., 2007, *A&A*, 461, 1209
 Dwelly T., Page M. J., 2006, *MNRAS*, 372, 1755
 Fabian A. C., 1999, *MNRAS*, 308, L39
 Fabian A. C., Celotti A., Erlund M. C., 2006, *MNRAS*, 373, L16
 Fabian A. C., Iwasawa K., 1999, *MNRAS*, 303, L34
 Fabian A. C., Wilman R. J., Crawford C. S., 2002, *MNRAS*, 329, L18
 Ferrarese L., Pogge R. W., Peterson B. M., Merritt D., Wandel A., Joseph C. L., 2001, *ApJ*, 555, L79
 Gebhardt K. et al., 2000, *ApJ*, 539, L13
 Giacconi R. et al., 2002, *ApJS*, 139, 369
 Hönig S. F., Beckert T., 2007, *MNRAS*, 380, 1172
 Kaspi S. et al., 2001, *ApJ*, 554, 216
 King A., 2003, *ApJ*, 596, L27
 Kollmeier J. A. et al., 2006, *ApJ*, 648, 128
 Kormendy J., Richstone D., 1995, *ARA&A*, 33, 581
 La Franca F. et al., 2005, *ApJ*, 635, 864
 Lawrence A., 1991, *MNRAS*, 252, 586
 Magorrian J. et al., 1998, *AJ*, 115, 2285
 Mainieri V., Bergeron J., Hasinger G., Lehmann I., Rosati P., Schmidt M., Szokoly G., Della Ceca R., 2002, *A&A*, 393, 425
 Maiolino R., Risaliti G., 2007, to appear in Ho L. C., Wang J. M., ed., *The Central Engine of Active Galactic Nuclei*, San Francisco (astro-ph/0701109)
 Marconi A., Hunt L. K., 2003, *ApJ*, 589, L21
 Markowitz A., Reeves J. N., Braito V., 2006, *ApJ*, 646, 783
 Markowitz A. et al., 2007, *ArXiv e-prints*, 710
 Markwardt C. B., Tueller J., Skinner G. K., Gehrels N., Barthelmy S. D., Mushotzky R. F., 2005, *ApJ*, 633, L77
 Mateos S., Barcons X., Carrera F. J., Ceballos M. T., Hasinger G., Lehmann I., Fabian A. C., Streblyanska A., 2005, *A&A*, 444, 79
 Matt G., 2000, *A&A*, 355, L31
 Murray N., Quataert E., Thompson T. A., 2005, *ApJ*, 618, 569
 Pier E. A., Krolik J. H., 1992, *ApJ*, 399, L23
 Simpson C., 1998, *MNRAS*, 297, L39
 Szokoly G. P. et al., 2004, *ApJS*, 155, 271
 Tozzi P. et al., 2006, *A&A*, 451, 457
 Treister E., Urry C. M., 2005, *ApJ*, 630, 115
 Tremaine S. et al., 2002, *ApJ*, 574, 740
 Ueda Y., Akiyama M., Ohta K., Miyaji T., 2003, *ApJ*, 598, 886
 van der Wel A., Franx M., van Dokkum P. G., Huang J., Rix H.-W., Illingworth G. D., 2006, *ApJ*, 636, L21
 Vasudevan R. V., Fabian A. C., 2007, *MNRAS*, 381, 1235